Orientation towards prey in antlions: efficient use of wave propagation in sand

Arnold Fertin* and Jérôme Casas

Université de Tours, IRBI UMR CNRS 6035, Parc Grandmont, 37200 Tours, France

*Author for correspondence (e-mail: arnold.fertin@etu.univ-tours.fr)

Summary

Substrate-borne vibration for locating mates, predators and prey is widespread in the animal kingdown. Antlion larvae dig funnel-shaped traps to catch ants and they are totally immersed in dry sand. We used a playback setup reproducing an ant walking on sand to clearly demonstrate that antlions use sand-borne vibrations to locate their prey. Half the tested animals moved towards the stimulus source. The shoot angle of sand tossing was very close to the target angle, indicating excellent ability to perceive stimulus direction. We also discuss orientation mechanisms in sand, a medium with highly unusual wave propagation properties.

Key words: Antlion trap, sit-and-wait predation, vibratory perception, orientation, physics of sand, wave propagation.

Introduction

Numerous arthropods use substrate vibrations to locate mates, predators and prey (Castellanos and Barbosa, 2006; Cocroft and Rodriguez, 2005; Elias et al., 2004; Greenfield, 2002; Mason et al., 2001). Whereas most insects studied use vibrations at the interface between a solid (often a plant) and air, some also use waves at the interface between water and air. Waterstriders and backswimmers are the most studied examples (Lang, 1980; Markl and Wiese, 1969; Markl et al., 1973; Murphey, 1971; Murphey and Mendenhall, 1971). However, we know very little about mechanical wave perception in insects completely imbedded in the substrate, including soil-dwelling arthropods and endophytic insects. Many different insects live embedded in substrate. Coupling between the insect and substrate should facilitate use of available mechanical information for orientation.

Antlion larvae are a good example of insects living in substrate, as they spend their life buried in sand. They are found in dry and sandy habitats and their larvae dig funnel-shaped pits to catch ants and other arthropods. The pits are dug starting from a circular groove, the antlion throwing sand with its mandibles. The antlion then gradually moves down spirally from the perimeter towards the centre, making the pit deeper and deeper (Tuculescu et al., 1987; Youthed and Moran, 1969). The antlion is at the trap centre when construction is complete, but may move away from the centre over time. The purpose of the antlion trap is to direct prey towards the bottom of the trap (Lucas, 1982). When the prey reaches the bottom of the pit, the antlion quickly closes its mandibles. This trap seems simple, but it requires a slope steep enough to convey prey while avoiding avalanches triggered by the inhabitant or by internal forces within the sand (Fertin and Casas, 2006). We have shown that antlions can construct pits with such an optimal slope.

Antlions prevent prey from escaping up the walls of the trap by throwing sand and attempting to bite them (Napolitano, 1998). Thus, the antlion predation can be more active than sit-and-wait predation. However, an active attack has higher energetic costs and much higher rebuilding costs as the antlion must rebuild the pit. Thus, as it is important that an active attack bring higher rewards, an antlion probably uses all available information for orienting its attack. We propose that the antlion orients its attack based on mechanical wave propagation through sand. Sand is made of large conglomerations of discrete macroscopic particles. Sand and other granular materials behave differently than the classic forms of solids, liquids and gases. Sand is a surprising medium which sometimes behaves as a liquid (avalanches) and sometimes behaves as a solid (Duran, 2000). Thus, it should be considered as a state of matter in its own right, in particular regarding mechanical wave propagation. Various animals use wave propagation in sand, including moles, vipers, lizards and scorpions (Brownell, 1977; Hetherington, 1992; Narins et al., 1997; Young and Morain, 2002). This study aimed to assess whether antlions use mechanical energy produced by struggling prey that is transmitted through sand to determine the direction and distance of prey. We also discuss the implications of sand properties in terms of orientation mechanisms.

Materials and methods

Wave propagation through sand caused by a walking ant

Signals transmitted through a layer of sand caused by an ant walking on the surface were measured. A condenser microphone (Brüel & Kjaer 4145, Mennecy, France) was used to measure changes in pressure of the sand in contact with a microphone membrane. The microphone was placed in a Plexiglas™ box (10.6 cm×10.6 cm×6 cm), which was filled with sand of calibrated granulometry (sand of Fontainebleau SDS190027, France; granulometry: 100–300 μm). The

membrane of the microphone was covered with 5 mm of sand and positioned parallel to the surface of sand (Fig. 1A). The signal from the microphone was amplified by a preamplifier (Brüel and Kjaer 2619) and an amplifier (Brüel and Kjaer 2608) with an 'A weighting network' filter (IEC 179-1965). The amplified signal was digitized by the sound entry of a graphics card (ADS Tech DVD Xpress, Cerritos, CA, USA). A camera (Panasonic Wv-bp130/G, Kadoma, Japan) was placed above the microphone and visual reference marks were placed on the box. These reference marks delimited the microphone membrane. The camera was connected to the video entry of the graphics card for proper synchronization of the microphone signal and the video recording. Workers of *Lasius fugilinosus* Latreille (Hymenoptera: Formicidae) were used because their carcasses were frequently observed around the traps in the field. An ant was placed on the surface of the sand for each recording. A signal from the microphone was produced when the ant walked between the visual reference marks. The number of leg strokes was determined from the video recording.

Reproducing ant walk

The aim was to create a biotest simulating the passage of an ant. The recording hardware was the same as described above. A walking ant was mimicked by a electromagnetic shaker (LDS V101, Ling Dynamic Systems, Royston, UK). The electromagnetic shaker was mounted on an aluminium rod with a 5 mm length needle at its end, which was in contact with the sand above the microphone membrane (Fig. 1B). A signal sent to the electromagnetic shaker by the sound card of the computer simulated the passage of an ant. The signal consisted of a series of pulses of frequency f. Each pulse was defined by a fragment of a high frequency sine curve (4 kHz):

$$d(t) = -k\sin(2\pi 4000 t) \quad t \in \left[0, \frac{1.5}{4000}\right],$$

where k is the signal amplitude in V. A pulse corresponds to the impact of the needle on sand. Goodness of pulse was checked using an oscilloscope. Recordings with the microphone were carried out at various amplitudes k. A power spectrum analysis was used to compare the recordings from ants with the recordings from the electromagnetic shaker. The pulse amplitude k was selected using this comparison of power spectra. An artificial stimulus of 150 s was then created, which simulated the walk of an ant on sand.

Behavioural bioassays

Second-stage larvae of *Euroleon nostras* Fourcroy (Neuroptera: Myrmeleontidae) were collected in Tours (47°21′16.36″N, 0°42′16.08″E, France). They were fed each day with ants and *Drosophila*. Thirty antlion larvae were placed in plastic boxes (10.6 cm×10.6 cm×6 cm) filled with Fontainebleau sand to a depth of 5 cm the day before the experiment to allow them to dig their traps during the night. The experiments were performed at controlled temperature, T (25.8±0.5°C), and moisture, RH (36.1±4.2%; means ± s.d.). The tip of the electromagnetic shaker was positioned carefully 10 mm behind the head of the antlion lying in its pit. The trap slope was between 29.61° and 37.60° (Fertin and Casas, 2006). Placing the tip 10 mm behind the antlion head gives a sand layer between 4.94 mm and 6.01 mm, similar to the sand layer used previously. Thus, the tip of the electromagnetic shaker was initially out of the reach of antlion mandibles. The stimulus simulating the walk of an ant was then produced.

Antlion attack behaviour during stimulation was recorded on camera (Euromex VC3031, Arnhem, Holland). Each video sequence was analysed frame by frame to quantify the attack behaviour, which consisted of attempted bites and sand tossing. Attacks were considered successful if the antlion had moved towards the tip of the electromagnetic shaker and bitten it. The distance from head to tip was measured in the first and the last frame. This measurement was used to calculate antlion displacement during stimulation.

The direction of sand tossing was measured in the frame corresponding to the moment the sand was tossed. A frame obtained with an analog camera consists of two interlaced half-images separated by 0.02 s (PAL format). The first half-image contains the odd lines and the second contains the even lines. A delay between the capture of the two half-images induces a difference of contrast typical of a moving object, called interlacing. The following procedure aims at sharpening these small contrast differences. We propose here a simple image processing method to detect the areas with interlacing (i.e. moving areas) in a frame corresponding to sand flying (Fig. 2A).

First, the frame was split into red, green and blue images using standard RGB channels. Blue images were not used because their noise levels were too high. The images were coded on a grey-scale level from 0 (white) to 255 (black). Second, the contrast difference was calculated:

$$\epsilon_{i,j} = \left| P_{i,j} - \frac{P_{i,j+1} + P_{i,j-1}}{2} \right| \quad \epsilon_{i,j} \in [0, \ 255].$$

If $P_{i,j}$ is close to the mean of grey values of the upper pixel $P_{i,j+1}$ and the lower pixel $P_{i,j-1}$, $\epsilon_{i,j}$ is close to 0. A pixel is therefore not interlaced if its grey value $P_{i,j}$ is close to the grey values of the upper pixel and the lower pixel. Third, the contrast
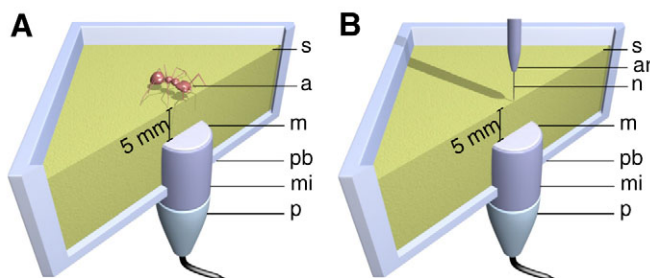

Fig. 1. (A) Schema of the setup to record wave propagation through sand caused by a walking ant. (B) Schema of the setup to simulate a walking ant with a electromagnetic shaker. s, sand; a, ant; mb, microphone membrane; pb, Perspex™ box; m, microphone; p, microphone preamplifier; ar, aluminium rod mounted on electromagnetic shaker; n, needle.
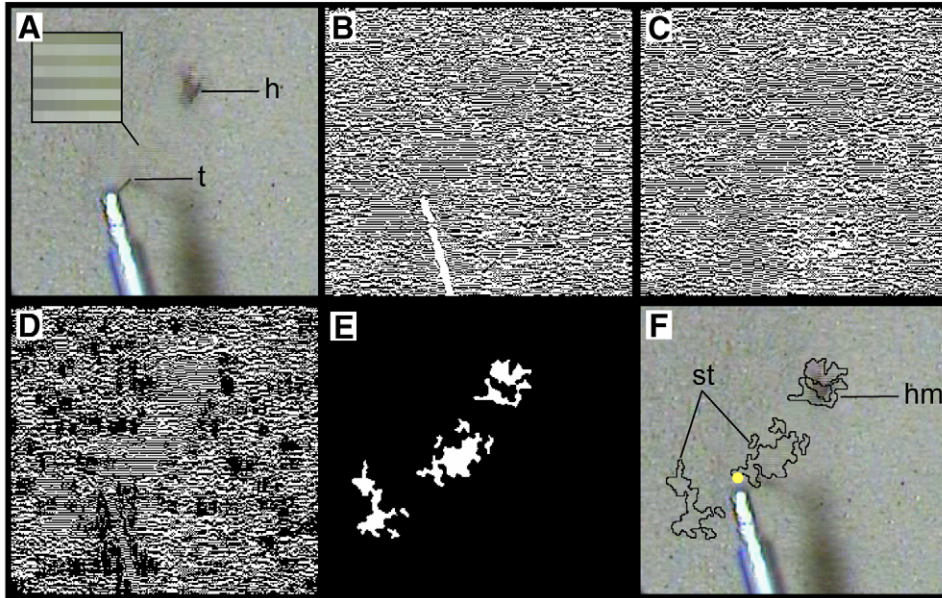
Fig. 2. Example of the detection algorithm of interlaced areas. See Materials and methods for further details. (A) Original frame with a close-up of an area with interlacing (boxed) in the upper left corner (contrast is enhanced for illustrative purposes). (B,C) First processing of red and green images. (D) Result of the Boolean 'AND' operation between red and green images. (E) Application of the despeckle filter after detection of interlaced area. (F) Final identification of moving areas during sand tossing relative to the source of stimuli. h, antlion head, t, tip of the electromagnetic shaker, hm, interlaced area due to head movement, st, interlaced areas due to flying sand. The yellow point is the centroid of sand tossing areas.

differences were simplified by applying the following binary threshold:

$$\begin{cases} \epsilon'_{i,j} = 0 & \text{if} \quad \epsilon_{i,j} \in [0, \ 1] \\ \epsilon'_{i,j} = 255 & \text{if} \quad \epsilon_{i,j} \in [1, \ 255] \end{cases}. \qquad \text{(i)}$$

This procedure was applied to the red and green images (Fig. 2B,C). Fourth, we combined the red and green images by applying the Boolean operation 'AND' between the red image and the green image. This operation keeps only the information that is identical in both images (Fig. 2D). Fifth, we defined the 3×3 window around a pixel $P_{i,j}$:

$$M = \begin{bmatrix} P_{i-1,j-1} & P_{i,j-1} & P_{i+1,j-1} \\ P_{i-1,j} & P_{i,j} & P_{i+1,j} \\ P_{i-1,j+1} & P_{i,j+1} & P_{i+1,j+1} \end{bmatrix}. \qquad \text{(ii)}$$

If a pixel is located in a region with interlacing, then the pattern of neighbouring pixels can be of two kinds only:

$$M_1 = \begin{bmatrix} 255 & 255 & 255 \\ 0 & 0 & 0 \\ 255 & 255 & 255 \end{bmatrix} \text{ or } M_2 = \begin{bmatrix} 0 & 0 & 0 \\ 255 & 255 & 255 \\ 0 & 0 & 0 \end{bmatrix}. \text{(iii)}$$

Thus, these pixels can be identified with the following operation:

$$\begin{cases} |M - M_1| = 0 \\ \text{or} \\ |M - M_2| = 0 \end{cases}. \qquad \text{(iv)}$$

Pixels $P_{i,j}$ outside interlaced areas were given the value of 255. Sixth, noise was removed with a despeckle filter of ImageJ (Abramoff et al., 2004) (a 3×3 median filter) (Fig. 2E). Seventh, the centroid of the sand flying area was computed. Sand tossing was defined by the centroid of the flying sand areas and its direction was measured in a reference frame centred on

the antlion head (Fig. 3). Precision of sand tossing was defined by the angle between the sand tossing and the tip of the electromagnetic shaker (α_3). As antlions moved during stimulation, we observed several angle values α_1 even though they were fixed at 90° at the start of the experiment. We took this movement into account in our analysis. Fifty sand tossings were randomly selected in the recording of 26 antlions (two sand tossings per individual on average) and analysed. ImageJ (Abramoff et al., 2004) was used to develop the algorithm for analysis.

Statistical analysis

Wilcoxon tests or Student's *t*-tests were used for statistical analyses of the differences in variables. The choice between these two tests was determined by the significance of the Shapiro–Wilk test for normality and *F* test for homoscedasticity. We used linear models for the correlation between certain variables, for which the significance of the correlation was assessed by *F* tests. Student's *t*-tests were used to analyse the significance of the parameters generated by these models. Rayleigh tests (Batschelet, 1981) were used to determine the significance of differences between the mean of circular variables and the 0° direction. The 95% confidence interval (CI; mean ± 95% CI) is indicated for all means and estimates.

Results
Estimation of biotest parameters

We observed recurrent signals from pressure recording for an ant walking above the microphone membrane (Fig. 4A). These signals had a shape similar to a damped oscillation (Fig. 4B). The mean of 20 signals randomly extracted in 15 recordings is shown in Fig. 4C. Mean signal recognition in recordings was performed with a normalized cross-correlation between pattern and recordings. The normalized cross-correlation function (CCF) is maximal when the recording is closest to the mean observed signal. Largest maxima of normalized CCF were detected as follows: (1) maxima of the
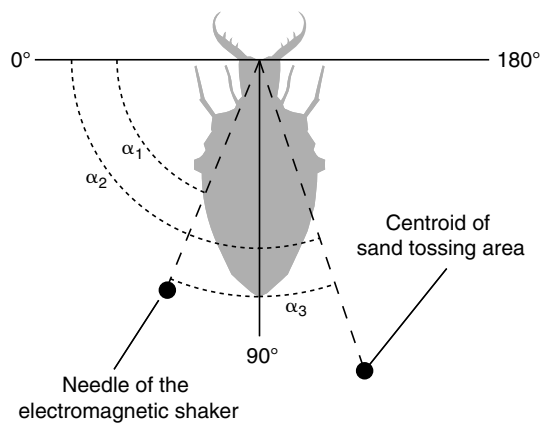
Fig. 3. Reference frame and angle definition. α_1, angle to the tip of the electromagnetic shaker; α_2, angle to sand tossing area; α_3, angle between tip location and sand tossing area, reflecting the precision of sand tossing.

f modelled by the electromagnetic shaker at 40 Hz. Pulse amplitude k was determined by recording pressure with several k values. We used spectral analysis of the electromagnetic shaker recordings to measure the power spectral density maxima for each k value. This value was a linear function of the amplitude k ($N=71$, $R^2=0.6554$, $P<0.001$). We used the k value that was equal to the mean of the maximal power spectral density extracted from 20 signals in the 15 ant recordings ($k=2.4$ V).

A mean signal was obtained from the mean of 20 signals extracted from electromagnetic shaker recordings as described above. Power spectral densities of mean signals for the ant pattern and the electromagnetic shaker pattern were very close, especially at the power peak (−19.75 dB at 1099 Hz for the ant pattern and −18.79 dB at 1059 Hz for the electromagnetic shaker pattern) (Fig. 5) (Norton and Karczub, 2003). The spectrum of the electromagnetic shaker pattern had a second, smaller peak at 4484 Hz, probably due to interference from the electromagnetic shaker or the attached needle.

Behavioral response to biotests

Twenty six of 30 antlions responded to the artificial prey. The behavioral responses were similar to complete attack behaviour in the presence of prey. Antlions tossed sand, attempted to bite the prey and moved towards the prey. The number of bites was not significantly different to the number of sand tossings (paired Wilcoxon signed-rank test, $N=26$, $V=107$, $P=0.0829$ We observed two types of bites: (1) a bite with a head movement towards the tip of the electromagnetic shaker, called a directed bite and (2) a bite with no head movement, called a non-directed bite. Non-directed bites occurred less frequently than directed bites (paired Wilcoxon signed-rank test, $N=26$, $V=0$, $P<0.001$). Thirteen antlions moved and bit the tip of the electromagnetic

normalized CCF were extracted by taking its derivative; (2) these maxima were smoothed with a cubic spline in order to eliminate small local peaks, leading to the production of an upper envelope; (3) the largest maxima of normalized CCF corresponding to the maxima of upper envelope extracted by taking its derivative. These largest maxima identify the timings of occurrence of a pattern within the records (Fig. 4D). The number of mean signals for each recording and the number of leg strokes during the recording were identical (Wilcoxon signed-rank test, $N=15$, $V=6$, $P=0.1094$). Thus the mean signal was equivalent to a leg stroke. We calculated the mean time between two mean signals for each recording: the mean rate of leg strokes was 40±9 Hz ($N=15$). Thus, we fixed the pulse rate
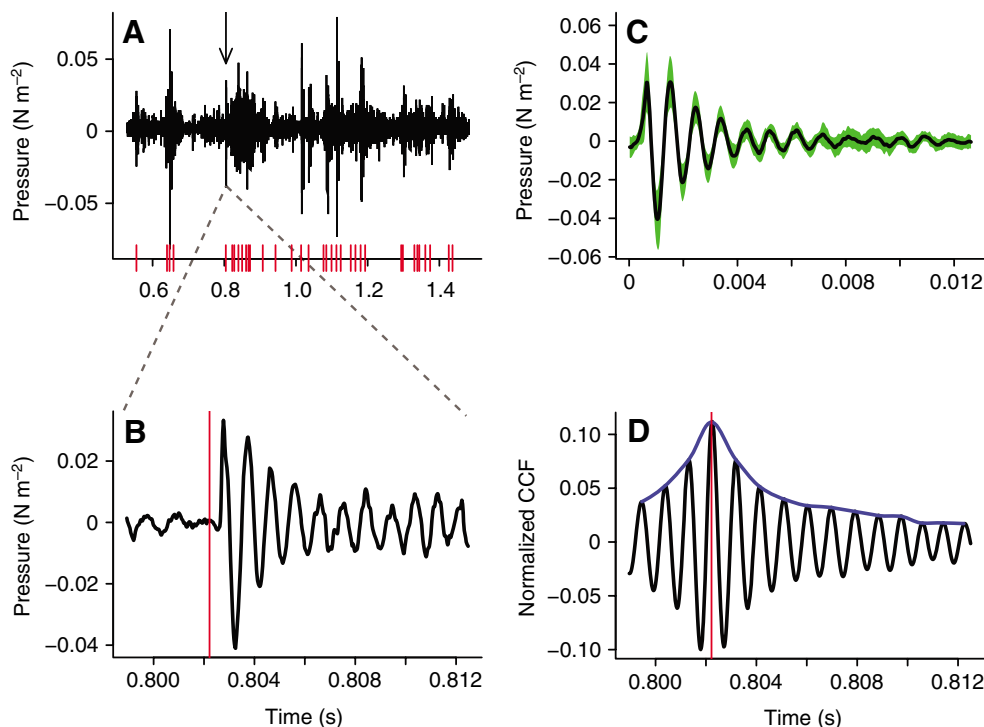

Fig. 4. Biotest design. (A) Example of a signal recorded when an ant walks on the sand surface above the membrane of the microphone. The arrow points to the signal reproduced in B; red lines represent leg strokes. (B) A close-up of the signal identified in the recording. (C) The mean signal used for pattern recognition. This signal was derived from the mean of 20 signals randomly extracted in 15 recordings. The green envelope indicates the standard deviation. (D) Example of pattern (i.e. mean signal) recognition in the recording shown in B. The blue curve is the smoothed envelope of the normalized cross-correlation function (CCF). The signals recognized using the maximum of the normalized cross-correlation function are indicated in B and D by vertical red lines.
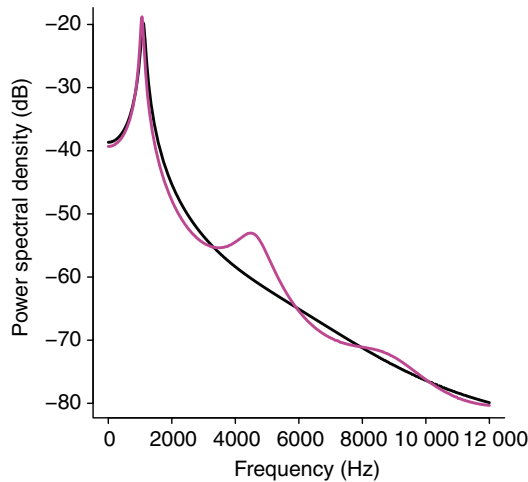
Fig. 5. Power spectral density comparison between the ant signal (black curve) and the electromagnetic shaker signal (pink curve).
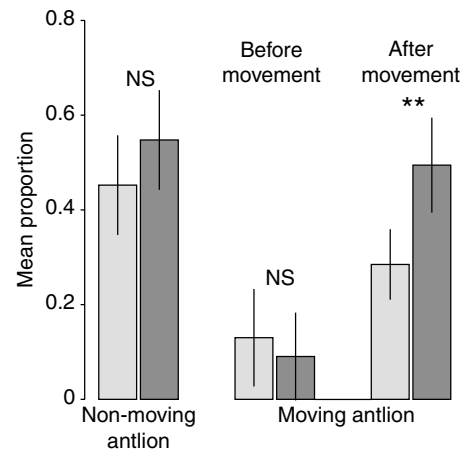

Fig. 6. Mean proportions of bites (light grey bars) and sand tossings (dark grey bars) during attacks by non-moving (left) and moving (right) antlions. Attacks by moving antlions were divided into two parts: before and after they started to move. Values are means ± 95% CI (paired Wilcoxon signed-rank test; non-moving: $N=13$, $V=34$, $P=0.4548$; before movement: $N=13$, $V=29$, $P=0.4961$; after movement: $N=13$, $V=9$, **$P<0.01$). NS, non-significant.

shaker. We considered these attacks successful (i.e. artificial prey was captured). The distance between the antlion head and the tip was shorter in the case of a successful attack than for a failed attack (5.15 ± 0.7 mm and 11.03 ± 0.93 mm, respectively, Student t-test, $N=26$, $t=11.2554$, $P<0.001$). This distance was shorter after successful attacks than at the start of the biotest (10 mm) (Student t-test, $N=13$, $t=-16.0474$, $P<0.001$). The probability of an antlion beginning its attack with sand tossing was significantly lower than 0.5 ($P=0.27\pm0.18$, binomial test, $P=0.0280$). Thus, an antlion often starts its attack with a bite. Non-moving antlions had the same proportion of bite and sand tossing in their attacks. By contrast, moving antlions used sand tossing more often, but only after they had started to move (Fig. 6).

The angular precision of sand tossing (α_3) was not significantly different from 0 (mean: $0.87\pm4.76°$, Rayleigh test, $N=50$, $r=0.9586$, $P<0.001$) (Fig. 7A). The angle of sand tossing (α_1) was a linear function of the angle of the electromagnetic shaker tip (α_2) ($N=50$, $R^2=0.5669$, $F=62.82$, $P<0.001$), with near perfect correlation (Rayleigh test, $N=50$, $r=0.9996$, $P<0.001$) (Fig. 7B). Thus, antlions throw sand in the direction of the stimulus.

Discussion

Antlions clearly responded to mechanical waves produced by struggling insects in their pits. Antlions did not adjust their behaviour according to the distance to their prey. They tried to bite prey that were out of reach and many did not move even after several attempts to dislodge them. The equal use of sand tossing and biting is another indication that they do not gauge distance to prey, even for those that moved later. Sand tossing that covers most of the distance to the pit edge dislodges prey or triggers avalanches that do the rest. Thus, it is not necessary for antlions to know the distance to their prey if they construct pits with an optimal slope that will bring prey to them (Fertin and Casas, 2006). By contrast, antlions estimated very well the direction of prey stimuli. The prominent use of directed bites and the nearly perfect sand tossing precision show that antlions
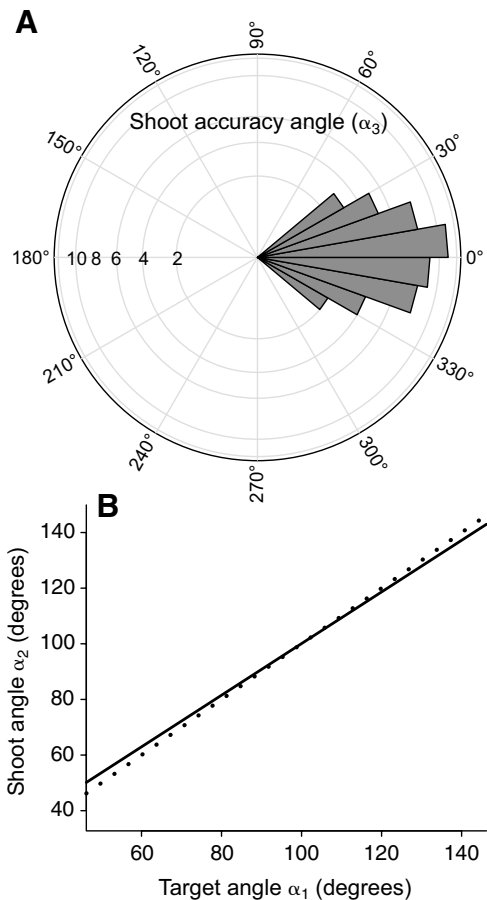

Fig. 7. (A) Circular distribution of the precision angle of sand tossings (α_3). The area of each sector is proportional to its frequency. The scale is indicated on the left half of the circle. (B) Angle of sand tossings (α_2) as function of the angle of the tip (α_1). This response is linear (solid line), and close to the perfect response (dotted line) (see text for details).

can extract directional information from mechanical waves. The movement of some antlions towards the tip of the electromagnetic shaker strengthens this conclusion.

The sensory physiology of antlions in relation to prey capture is unknown except for the work of Devetak (Devetak, 1985), in which an antlion was stimulated to leave its pit in a highly contrived manner. *Euroleon nostras* have six pairs of stemmata with about 45 receptors and a lens aperture of 60 μm. The temporal and spatial resolution of these stemmata are coarse (flicker fusion frequency=27 Hz, acceptance angle=8°, total receptor field=47°) (Jockusch, 1967; Gilbert, 1994; Land and Nilson, 2002). In our experiments, the needle was fine (150 μm), and the time of needle movement for each pulse was short (0.375 ms). Antlions reacted only when the needle was set into vibratory motion. Therefore, vision was not involved in prey capture in our study. Vision may possibly be used to supplement mechanical information, e.g. about distance, in the presence of real prey.

The responses clearly show that antlions detect their prey through wave propagation in sand. The use of sand as a transmission medium for mechanical information has been studied with scorpions and crabs (Aicher and Tautz, 1989; Brownell, 1977; Browell and Farley, 1979). Sand scorpions assess prey direction in the same sandy environment with even better accuracy of orientation than antlions. Sand scorpions have eight vibration receptors on tarsi. A neuronal model explains how these sensors work (Brownell and van Hemmen, 2001; Stürzl et al., 2000). Various authors have claimed that scorpions use Raleigh surface waves. However, antlions cannot use Rayleigh waves as easily because they are totally immersed in sand. Measurements of Rayleigh waves decay within sand will be necessary to clarify this point. They are transmitted to some depth within the substrate and antlions live in a subsurface layer.

Wave propagation within granular materials has been studied only recently (Liu and Nagel, 1992; Somfai et al., 2005) and even more recently in sand (Bonneau et al., 2007). In a granular medium, waves travel along specific paths determined by the geometrical arrangement of sand grains, which itself defines a contact network between grains. Thus, Liu and Nagel showed that transmission is dominated by strong spatial fluctuations of force networks (Liu and Nagel, 1992). Consequently, the slightest temperature change induces major rearrangements of forces and sometimes a great loss of transmission. This exceptional sensitivity was shown by Liu and Nagel (Liu and Nagel, 1993). An increase of 1°C in a glass bead decreases transmission of sound within a layer of beads by 50%. Thus, wave propagation in sand, once considered at the microscale of reception, is not understood, except that it entails a large amount of stochasticity. The nearly perfect directional orientation of antlions buried in sand is therefore most remarkable given the high degree of unpredictability in the force networks within the medium. These two facts imply that antlions integrate the information in waves produced by struggling prey over many receptors distributed over a large portion of their body surface. The exact nature of the waves they use for orientation is unknown, as is our understanding of wave propagation in this unique animal construction.

List of symbols and abbreviations

CCF	cross-correlation function
$d(t)$	equation of pulse as a time function
f	pulse rate
k	pulse amplitude
M	three by three window around $P_{i,j}$
M_1, M_2	pattern of neighbouring pixels
$P_{i,j}$	pixel value at (i,j) coordinates
α_1	target angle
α_2	shoot angle
α_3	shoot accuracy angle
$\epsilon_{i,j}$	contrast difference
$\epsilon_{i,j}'$	contrast difference after thresholding

References

Abramoff, M. D., Magelhaes, P. J. and Ram, S. J. (2004). Image processing with ImageJ. *Biophoton. Int.* **11**, 36-42.

Aicher, B. and Tautz, J. (1989). Vibrational communication in the fiddler crab, *Uca pugilator. J. Comp. Physiol. A* **166**, 345-353.

Batschelet, E. (1981). *Circular Statistics in Biology*. London: Academic Press.

Bonneau, L., Andreotti, B. and Clément, E. (2007). Surface elastic waves in granular media under gravity and their relation to booming avalanches. *Phys. Rev. E* **75**, doi: 10.1103/PhysRevE.75.016602.

Brownell, P. H. (1977). Compressional and surface waves in sand: used by desert scorpions to locate prey. *Science* **197**, 497-482.

Brownell, P. H. and Farley, R. D. (1979). Orientation to vibrations in sand by the nocturnal scorpion *Paruroctonus mesaensis*: mechanism of target localization. *J. Comp. Physiol. A* **131**, 31-38.

Brownell, P. H. and van Hemmen, J. L. (2001). Vibration sensitivity and a computational theory for prey-localizing behavior in sand scorpions. *Am. Zool.* **41**, 1229-1240.

Castellanos, I. and Barbosa, P. (2006). Evaluation of predation risk by a caterpillar using substrate-borne vibrations. *Anim. Behav.* **72**, 461-469.

Cocroft, R. B. and Rodriguez, R. (2005). The behavioral ecology of insect vibrational communication. *BioScience* **55**, 323-334.

Devetak, D. (1985). Detection of substrate vibrations in the antlion larva, *Myrmeleon formicarius* (Neuroptera: Myrmeleonidae). *Bioloski Vestnik* **33**, 11-22.

Duran, J. (2000). *Sands, Powders and Grains: An Introduction to the Physics of Granular Materials*. New York: Springer-Verlag.

Elias, D. O., Mason, C. A. and Hoy, R. R. (2004). The effect of substrate on the efficacy of seismic courtship signal transmission in the jumping spider *Habronattus dossenus* (Araneae: Salticidae). *J. Exp. Biol.* **207**, 4105-4110.

Fertin, A. and Casas, J. (2006). Efficiency of antlion trap construction. *J. Exp. Biol.* **209**, 3510-3515.

Gilbert, C. (1994). Form and function of stemmata in larvae of holometabolous insects. *Annu. Rev. Entomol.* **39**, 323-349.

Greenfield, M. D. (2002). *Signalers and Receivers: Mechanisms and Evolution of Arthropod Communication*. Oxford: Oxford University Press.

Hetherington, T. E. (1992). Behavioral uses of seismic cues by the sandswimming lizard *Scincus scincus. Ethol. Ecol. Evol.* **4**, 5-14.

Jockusch, B. (1967). Bau und Funktion eines larvalen Insektenauges. Untersuchungen am Ameisenl6wen *(Euroleon nostras,* Planipennia: Myrmeleontidae). *Z. Vgl. Physiol.* **56**, 171-198.

Land, M. F. and Nilsson, D. E. (2002). *Animal Eyes*. Oxford: Oxford University Press.

Lang, H. H. (1980). Surface wave discrimination between prey and non prey by the back swimmer *Notonecta glauca* L. (Hemiptera, Heteroptera). *Behav. Ecol. Sociobiol.* **6**, 233-246.

Liu, C. H. and Nagel, S. R. (1992). Sound in sand. *Phys. Rev. Lett.* **68**, 2301-2304.

Liu, C. H. and Nagel, S. R. (1993). Sound in a granular material: disorder and nonlinearity. *Phys. Rev. B* **48**, 15646-15650.

Lucas, J. R. (1982). The biophysics of pit construction by antlion larvae. *Anim. Behav.* **30**, 651-657.

Markl, H. and Wiese, K. (1969). Die empfindlichkeit des rückenswimmers *Notonecta glauca* L. for oberflächenwellen des wassers. *Z. Vgl. Physiol.* **62**, 413-420.

Markl, H., Lang, H. and Wiese, K. (1973). Die genauigkeit der ortung eines wellenzentrums durch den rückenswimmer *Notonecta glauca* L. *J. Comp. Physiol. A* **86**, 359-364.

Mason, M. J. and Narins, P. M. (2001). Seismic signal use by fossorial mammals. *Am. Zool.* **41**, 1171-1184.

Murphey, R. K. (1971). Sensory aspects of the control of orientation to prey by the waterstrider, *Gerris remigis*. *J. Comp. Physiol. A* **72**, 168-185.

Murphey, R. K. and Mendenhall, B. (1971). Localization of receptors controlling orientation to prey by the backswimmer *Notonecta undulata*. *J. Comp. Physiol. A* **84**, 19-30.

Napolitano, J. F. (1998). Predatory behaviour of pit-making antlion, *Myrmeleon mobilis* (Neuroptera: Myrmeleontidae). *Fla. Entomol.* **81**, 562-566.

Narins, P. M., Lewis, E. R., Jarvis, J. J. U. M. and O'Riain, J. (1997). The use of seismic signals by fossorial southern African mammals: a neuroethological gold mine. *Brain Res. Bull.* **44**, 641-646.

Norton, M. P. and Karczub, D. G. (2003). *Fundamentals Noise and Vibration Analysis for Engineers*. Cambridge: Cambridge University Press.

Somfai, E., Roux, J. N., Snoeijer, J. H., van Hecke, M. and van Saarloos, W. (2005). Elastic wave propagation in confined granular systems. *Phys. Rev. E* **72**, 021301.

Stürzl, W., Kempter, R. and van Hemmen, J. L. (2000). Theory of arachnid prey localization. *Phys. Rev. Lett.* **84**, 5668-5671.

Tuculescu, R., Topoff, H. and Wolfe, S. (1975). Mechanism of pit construction by antlion larvae. *Ann. Entomol. Soc. Am.* **68**, 719-720.

Young, B. A. and Morain, M. (2002). The use of ground-borne vibrations for prey localization in the Saharan sand vipers (*Cerastes*). *J. Exp. Biol.* **205**, 661-665.

Youthed, G. J. and Moran, V. C. (1969). Pit construction by myrmeleontid larvae. *J. Insect Physiol.* **15**, 867-875.